Streak camera for picosecond x-ray diagnostics

P. A. Jaanimagi[a] and M. C. Richardson[b]

Division of Physics, National Research Council of Canada, Ottawa, Canada K1A 0R6

(Received 27 December 1982; accepted for publication 10 May 1983)

We report details of an x-ray sensitive streak camera with an estimated time resolution of less than 10 ps. The streak camera is based on a modified RCA 73435 image tube and features a large photocathode area and high sensitivity. A direct comparison of the relative quantum efficiency of Au and CsI photocathodes for 1–10 keV x rays is also presented.

PACS numbers: 07.85. + n, 07.68. + m, 42.80.Qy, 85.10.Pe

INTRODUCTION

The first x-ray sensitive streak cameras were developed in the mid-1970's concurrently at several laboratories.[1] Much of the incentive for developing these devices stemmed from their potential and versatility in diagnosing the x-ray emission from high-power laser produced plasmas. The interest in x-ray sensitive cameras also developed naturally from efforts to extend the spectral sensitivity of ultrafast streak camera systems. The first x-ray streak tubes were virtually identical to their visible light sensitivity counterparts as two basic approaches were used to facilitate their fabrication. One was simply to replace the visible photocathode with an x-ray transmitting substrate (usually Be foil) bearing a photocathode sensitive to x rays in the 1–20-keV range. Alternatively a solid x-ray sensitive surface was placed in the photocathode plane and illuminated with electron-optic x rays at grazing incidence from the side. However, the performance of these devices with electron optics based on existing electron-optic shutter tube designs suffered from limitations created by the transition from optical to x-ray operation.

The primary limiting factor in the time-resolution capability of all streak cameras is the time-of-flight dispersion of the photoelectrons, due to a finite spread in their initial energies ($\Delta\epsilon$). For visible light sensitivity photocathodes $\Delta\epsilon$ is < 1 eV, (Ref. 2). The corresponding time-resolution limit, governed primarily by the accelerating field at the cathode, is typically a few picoseconds for modern streak tubes. In comparison $\Delta\epsilon$ for x-ray sensitive photocathodes is determined by the secondary electron emission characteristics and is, therefore, several electron volts.[3,4] Thus for similar accelerating field conditions the time-of-flight dispersion for these first x-ray streak tubes was several tens of picoseconds.

This limitation in time-resolution capability is not the only problem encountered in the simple conversion of ultrafast streak camera operation from the visible spectrum to the x-rays region. The high-energy (~ 1 keV) photons intercepted by the x-ray photocathode can cause a number of undesirable subsidiary effects. For streak tubes with transmission-type photocathodes, the majority of the x rays pass straight through the photocathode and can induce significant fluorescence from the phosphor of the tube. An additional problem for x-ray streak tubes is secondary electron emission caused by x rays and high-energy photoelectrons impinging on other electrode surfaces, such as the accelerating grid. This can produce ghost images or at least reduce signal-to-noise levels.

The standard visible streak tube design also has other disadvantages. The small photocathode area (8-mm diam.) utilized in many tubes limits the number of effective resolution elements across the photocathode. As well, most streak tubes have an electron-optical magnification greater than 1.0 which leads to a reduced dynamic range in ultrafast operation. This is based on space-charge considerations as will be shown.

I. ELECTRON-OPTICAL STREAK TUBE DESIGN

Keeping the limitations mentioned above in mind, a development program was initiated to determine to what extent an existing electron-optical tube could be modified to improve its performance as an x-ray sensitive device. Specifically, we wished to devise an x-ray streak camera system having the highest possible time resolution, preferably less than 10 ps. In that its intended use was for time-resolved studies of the x-ray emission from laser produced plasmas, the streak camera should have a large number of spatial resolution elements permitting its effective incorporation with imaging or spectrographically resolving systems. It should have high sensitivity, employing photocathodes with large quantum efficiency and low noise characteristics, since in general x-ray fluence is at a premium. In addition, the tube was to remain unsealed with a demountable cathode assembly to permit flexibility in replacing photocathodes. Ease of operation and simplicity were facilitated by incorporating the tube within the vacuum vessel in which the laser-target experiments were performed. This reduced the complexity of the vacuum system required for the streak tube, but demanded that all experiments were performed at pressure $< 10^{-5}$ Torr.

The RCA 73435 image tube[5] was selected as the basic design to be modified. This tube in its original form with a visible light sensitivity cathode has a demonstrated time resolution of ~ 5 ps, (Ref. 6) and a dynamic range (at this time resolution) which is higher than other commercially available streak tubes.[7] It has a large photocathode area with acceptable spatial resolution, and an open wire grid providing low secondary electron noise and large photoelectron throughput.

It has also been reported that the RCA tube exhibits nonlinear electron-optical magnification as the field at the cathode is increased.[8] This nonlinearity is such that as the

accelerating field is increased the magnification along the slit length increases to slightly above unity, while in the direction of the slit width the electron lens demagnifies the image by a factor of 3–5. In redesigning the tube the accelerating field at the cathode was increased to decrease the time-of-flight dispersion. The resulting spatial demagnification in the streak direction permitted wider input slits to be used, thereby increasing the solid angle subtended at the source by the photocathode and consequently the incident x-ray flux and overall camera sensitivity.

Demagnified electron optics is also a desirable feature in a streak tube for dynamic range considerations. This is with regard to space-charge broadening of the photoelectron current pulse in the photocathode region where the electrons travel slowly and the charge density is large.[6,9] With demagnifying electron optics one can increase the cross-sectional area of the initial photoelectron beam, yet produce an identical image size on the phosphor screen. Therefore, for the same limiting charge density one can draw more total current from the photocathode and thus improve the dynamic range. Similar arguments also hold for space-charge broadening in the focusing region.[10] Consideration of this region is important as $\sim\frac{1}{3}$ of the total transit time (cathode to phosphor) is spent in this section (which is at only $\sim 10\%$ of the cathode-to-anode potential). Alternatively, demagnification allows one to increase the current density at the phosphor screen, thereby reducing the low-intensity threshold and/or image intensifier gain requirements for recording the streaked image.

A schematic of the electrode configuration for the new x-ray streak tube is presented in Fig. 1. The major modifications were made in the front-end electrodes. The cathode electrode consisted of a stainless-steel plate with a 10-cm-radius concave inner surface, and was simply attached to the tube housing with four screws for fast and easy disassembly. The slit defining the photocathode area was cut in this plate and the photocathode substrate (12-μm Be) was glued with silver loaded epoxy to the inside of the plate. The slit measuring 1.3×25.4 mm was positioned 4.5 mm from the tube axis to eliminate the "straight through" x rays from reaching the phosphor screen. An extension was added to the grid cone to enable increasing the accelerating field at the cathode. This extension had an aperture 38 mm in diameter, and an open grid of 400-μm-wide ribbon wire was formed on it over a spherical mandrel to match the cathode curvature. Six grid wires on 4.5-mm centers were placed symmetrically about the tube axis and the photocathode slit. The cathode-to-grid separation was 2.3 mm and the accelerating field at the center of the photocathode could now be increased to over 12.5 kV/cm. The other electrodes were not modified. The streak deflection circuitry comprised a double stack of avalanche transistors (2N3700, seven per stack) for two sided deflection, electrically triggered with a 10-V signal generated in synchronism to the laser produced event to be studied. This circuit had a jitter of less than $\pm$ 50 ps and generated a voltage transient with $dV/dt \sim 1$ kV/ns to provide streak speeds up to 3.3×10^9 cm/s with a linearity of $\pm$ 5%. The recording system consisted of a proximity focused channel plate image intensifier (gain of 5000) fiber-optically coupled to the streak camera phosphor screen through a 50–25-mm fiber-optic taper. The streaked images were recorded on either Polaroid-type 47 or Kodak 2475 negative film.

To facilitate focusing and testing of the x-ray streak tube a small continuous flux x-ray source was built. This is shown schematically in Fig. 2. It consisted of an electron source (thermionic emission from a heated tungsten filament) which was geometrically focused onto the point of the anode at < 20 kV potential situated inside a grounded cylinder 12-mm diam. X rays were produced as bremsstrahlung and line radiation from the electrons bombarding the copper anode. It was found that with the x-ray source 20 cm from the photocathode of the streak camera an anode current of 100 μA at 10 kV produced more than sufficient x rays to visually observe the photocathode image on the phosphor.

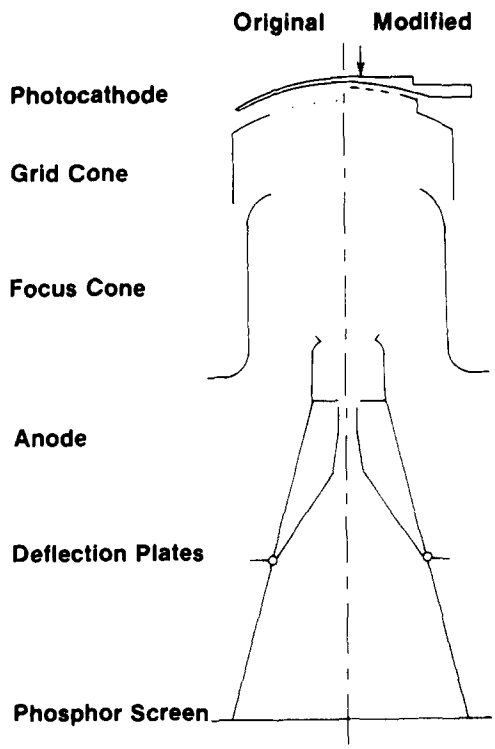

FIG. 1. Schematic of the cross section of the electrode configuration of original and modified streak tubes. Arrow shows photocathode slit position.

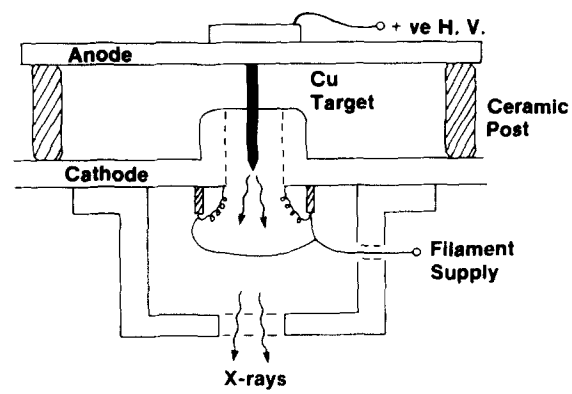

FIG. 2. Schematic of dc x-ray source.

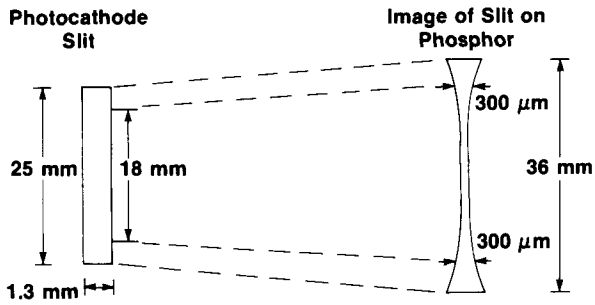

FIG. 3. Diagram detailing nonlinear electron-optical magnification of the slit image.

Static performance of the streak tube design was evaluated with the aid of this x-ray source. The maximum accelerating field at the photocathode was limited to 8.5 kV/cm by the focusing capability of the unmodified electrodes to compensate for the negative lens created by the grid wires. As in all crossover-type electron-optic tubes the image quality is best in the paraxial region and deteriorates both towards the edge of the streak record and the ends of the slit. The nonlinear electron-optical magnification was clearly evident for large (8.5 kV/cm) accelerating field. The image of the 25-mm slit length was magnified by a factor of 1.44. However, the image of the 1.3-mm-wide slit was demagnified to less than 300 μm over a region encompassing the central 18-mm-long section of the slit and 3 cm of the streak record at the phosphor, Fig. 3. By narrowing the slit the width of the image could be reduced further, but at the expense of overall sensitivity. The spatial resolution along the slit length was ~ 100 μm.

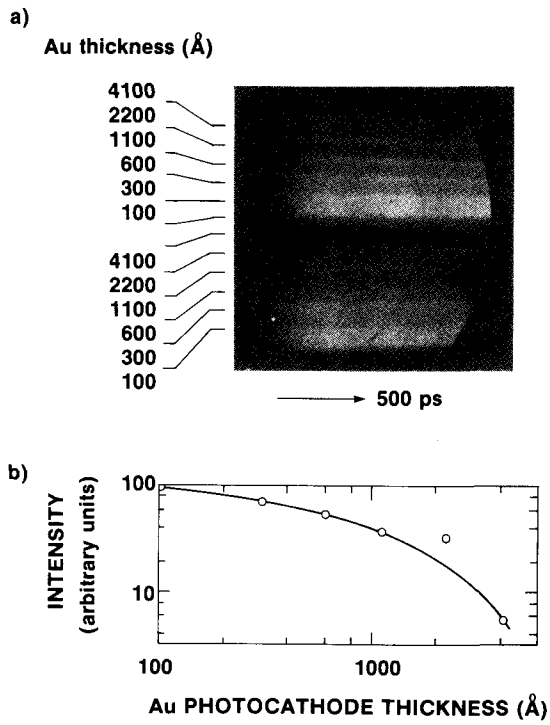

FIG. 4. (a) Streak record of x-ray emission from Al target with stepped Au photocathode. (b) Recorded intensity vs Au thickness.

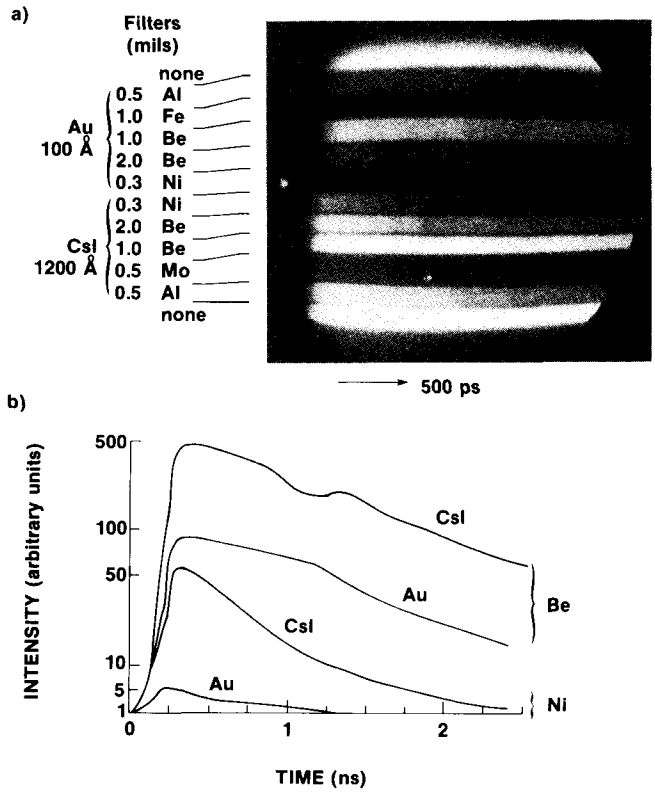

FIG. 5. (a) Streak record of x-ray emission from Cu target using composite Au/CsI photocathode. The cathode slit was covered with a set of absorber foil filter to allow comparisons in different spectral regions. (b) Densitometer traces for 8-μm Ni and 25-μm Be channels. The dip in the densitometer trace for CsI (Be channel) at 1.0–1.25 ns is due to a localized decrease in sensitivity in the image intensifier.

Dynamic performance of the new x-ray streak tube was evaluated using the broadband x-ray spectrum emitted from a laser-produced plasma and is illustrated in Figs. 4 and 5. The clarity of the streak records demonstrates a workable tube; the isolation of the channels attests to good spatial resolution along the slit. These streaked images record the time history of the x-ray emission (1–10 keV), 90° to target normal, produced by the COCO II laser at $I \sim 10^{14}$ W/cm^2 on microdisk targets of Al and Cu, respectively.[11] The COCO II laser is a CO_2 laser system delivering 20 J on target in a 1-ns pulse. The photocathode-to-target distance was 35 cm and the streak speed was 1.6×10^9 cm/s. The intensity scales in Figs. 4(b) and 5(b) were derived from density versus log E curves for the recording film exposed with blue light through a neutral density step wedge.

II. PHOTOCATHODE SENSITIVITY STUDIES

The photoelectron energy spectrum emitted from x-ray photocathodes is distinctly different from that for visible light sensitivity photocathodes. The x-ray photon generated electrons can be divided into two basic groups: primary photoelectrons ejected from the K, L, M... levels and Auger electrons; and low-energy (< 10 eV) secondary electrons. These secondary electrons are generated through various collisional processes as the primaries traverse through the cathode. The dominant photoemission current is that of secon-

dary electrons and it is upon these that the detection system is based. Recently, the physics of secondary electron generation and energy distributions for low-energy x rays have been investigated through the work of Henke *et al.*[3,12]

The quantum efficiency, or the ratio of the number of secondary electrons emitted from a transmission photocathode to incident x-ray flux, depends on many factors which include: (1) the x-ray transmission through the cathode substrate, (2) the photocathode thickness, (3) the range of the primary and secondary electrons in the photocathode, (4) the x-ray absorption efficiency of the photocathode, and (5) the x-ray photon energy and various bulk characteristics of the photocathode material. Good photocathode quantum efficiency results if the primary electron energy is effectively deposited in the photocathode layer within the secondary electron range of the emission surface. Therefore, the optimum thickness of the cathode is a compromise between this electron range and the x-ray absorption lengths; thin photocathodes have poor response due to the decreased x-ray absorption efficiency and a thick cathode will attenuate the x-ray flux prior to the emission volume.

The optimum Au photocathode thickness for sensitivity to 1–10-keV x rays was investigated using a stepped photocathode. This cathode consisted of a double set of six thicknesses of Au ranging from 100 to 4100 Å. Each step was ~2-mm wide with a few hundred micron gap between each step and a ~1-mm space between sets. Each thickness was evaporation deposited in a single layer except for the 2200-Å thickness which was done as a double layer of 1100-Å thickness with the vacuum broken in between. A streak record of the x rays from the COCO II laser irradiated Al target using this stepped cathode is presented in Fig. 4(a). The dominant recorded x-ray emission is in the 0.8 to 1.5-keV spectral region. The 12-μm Be substrate cuts off the lower-energy x rays. The combination of longer x-ray attenuation lengths and decreasing x-ray flux results in poor streak camera sensitivity at higher energies. A plot of the sensitivity or recorded intensity versus Au thickness is presented in Fig. 4(b). The optimum Au thickness was found to be 100 Å in agreement with Stradling *et al.*[13] who used 500-eV x rays and with theoretical predictions by Henke.[3]

A variety of other x-ray photocathode materials[3] have been investigated with the aim of increasing the secondary electron yields. Of particular interest is CsI. CsI has a small secondary electron energy spread and, therefore, better time resolution should result from the decreased time-of-flight dispersion. To make a direct comparison of the relative sensitivities of CsI and Au a composite photocathode was fabricated, half of which was 100-Å Au and the other half 1200-Å CsI. The streak camera photocathode slit was covered with two similar sets of K-edge absorber foil filters to permit comparisons in different spectral regions. The streak record and the corresponding densitometer traces of the channels filtered with 8-μm Ni and 25-μm Be are presented in Fig. 5, for x-ray emission emanating from a plasma produced off a Cu target by the COCO II laser. The increased sensitivity of CsI over Au for the Ni and Be channels (x-ray spectrum above 4 and 1 keV, respectively) was ~10 and 5, respectively. The peak recorded intensity of the unfiltered CsI channel was over 1000 above film fog levels and this was deemed sufficient to allow time-resolved x-ray imaging of the plasma with this camera.[14,15]

III. TEMPORAL RESOLUTION OF THE STREAK CAMERA

Direct measurements of the time resolution of an x-ray streak camera requires a quasimonochromatic burst of x rays a few picoseconds in duration. Such a source, with sufficient brightness in the 1–10-keV energy range has not yet been reported. An alternative approach is to estimate the time resolution using a digital analysis of the electron optics in the tube. This involves numerically estimating the potential distribution inside the streak tube and then calculating the resulting electron trajectories.

The electrostatic potential distribution was determined numerically by iteratively solving a finite difference analog of Laplace's equation for the potentials and geometry of the various electrodes used in the tube, together with appropriate boundary conditions for the interelectrode spaces.[16] One quadrant of the streak tube volume was simulated with a 3D mesh of nonuniform spacing; the spacing being smallest near electrode boundaries, the grid wires, and the tube axis. The finite difference equation

$$V_0^{n+1} = (1 - W)V_0^n + \frac{W\left[\Sigma_i (S_{i+} + S_{i-})^{-1}(V_{i+}/S_{i+} + V_{i-}/S_{i-})\right]}{\Sigma_i (S_{i+} S_{i-})^{-1}}$$

was solved at each mesh point with a new value of V_0 replacing the previous one. $S_{i+/-}$ are the distances from the mesh point under consideration to the neighboring points at potential $V_{i+/-}$ in the $+/-$ directions, respectively, $i = x, y, z$ and n is the iteration count. W is an acceleration factor to speed up the rate of convergence of the solution.[17]

A plot of the calculated axial potential in the streak tube for the operating electrode potentials ($V_K = 0$, $V_G = 3.1$ kV, $V_F = 840$ V, $V_A = 17$ kV) is presented in Fig. 6(b). The accelerating field at the center of photocathode was 8.55 kV/cm, gradually increasing toward the edges and along the length of the slit. However, uniformity of the extraction field is better than 2.5% over the full photocathode area. The equation of motion for the simple electron trajectory along the tube axis where the traverse fields are zero was numerically integrated. A plot of the relative time-of-flight dispersion versus initial electron energy is presented in Fig. 6(a). Using Henke's data for the initial secondary electron energy distribution [$\Delta\epsilon$ (Au) = 3.5 Ev, $\Delta\epsilon$ (CsI) = 1.7 eV] the time-of-flight dispersions are 9.5 and 6.0 ps for the Au and CsI photocathodes, respectively. By narrowing the slit or increasing the streak speed to decrease the technical time resolution to

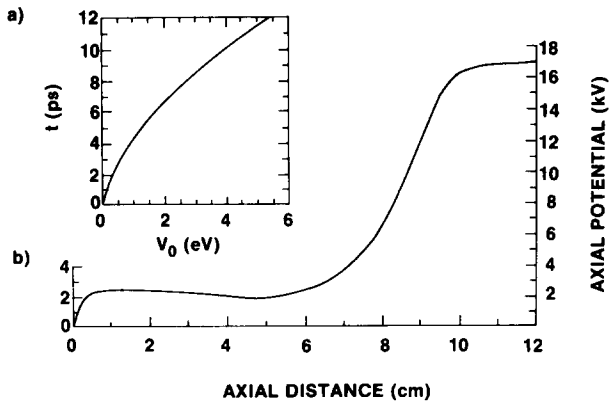

FIG. 6. (a) Plot of relative time-of-flight dispersion for electron trajectories along the streak tube axis for the axial potential presented in (b). V_0 is the initial photoelectron energy.

below 8 ps, an instrumental time resolution of < 10 ps should be achievable with this x-ray streak tube when using a CsI photocathode.

IV. DISCUSSION

We have successfully modified an existing streak tube design to incorporate a large area, x-ray sensitive photocathode and demagnified electron optics, resulting in high sensitivity and large dynamic range. The new front-end electrode design eliminates the noise due to secondary electron emission generated by photoelectrons and x rays intercepting these electrodes as well as the problem of phosphor fluorescence induced by directly transmitted x rays. The estimated time-resolution capability for this x-ray streak tube is less than 10 ps. Photocathode quantum efficiency was also improved for 1–10-keV x rays by utilizing CsI as the photocathode material.

ACKNOWLEDGMENT

We gratefully acknowledge R. W. Sancton for his excellent technical support with the streak camera.

[a] Present address: Department of Physics, University of Hawaii at Manoa, Honolulu, Hawaii 96822
[b] Present address: University of Rochester, Laboratory for Laser Energetics, 250 East River Road, Rochester, New York, 14623

[1] C. F. McConaghy and L. W. Coleman, Appl. Phys. Lett. **25**, 268 (1974); G. I. Brukhnevitch, V. K. Chevoklin, Yu. S. Kasyanov, V. V. Korobkin, A. A. Malyutin, A. M. Prokhorov, M. C. Richardson, M. Ya. Schelev, and B. M. Stepanov, Phys. Lett. A **51**, 249 (1975); D. J. Bradley, A. G. Roddie, W. Sibbet, M. H. Key, M. J. Lamb, C. L. S. Lewis, and P. Sachenmaier, Opt. Commun. **15**, 231 (1975).
[2] N. A. Soblev, A. G. Berkovsky, N. O. Chechik, and R. E. Eliseev, *Photoelectronic Devices* (Science, Moscow, 1965), p. 124; "Fundamental Photosurface Studies," USA ERDL Night Vision Lab, Fort Belvoir, 1966.
[3] B. L. Henke, J. Liesegang, and S. D. Smith, Phys. Rev. B **19**, 3004 (1979).
[4] Initial estimates of $\Delta\epsilon$ for Au cathodes for 1-keV x rays ranged from 25 to 240 eV, see papers in Ref. 1.
[5] R. G. Stoudenheimer and J. C. Moor, RCA Rev. **18**, 322 (1957).
[6] M. Ya. Schelev, M. C. Richardson, and A. J. Alcock, Rev. Sci. Instrum. **43**, 1819 (1972).
[7] S. W. Thomas and G. E. Phillips, Proc. 12th Inter. Cong. on High Speed Photography and Photonics, SPIE **97**, 11 (1977).
[8] S. W. Thomas and G. E. Phillips, Proc. 13th Inter. Cong. on High Speed Photography and Photonics, SPIE **189**, 471 (1979).
[9] D. J. Bradley, S. F. Bryant, J. R. Taylor, and W. Sibbett, Rev. Sci. Instrum. **49**, 215 (1978).
[10] H. Niu and W. Sibbett, Rev. Sci. Instrum. **52**, 1830 (1981).
[11] M. C. Richardson, N. H. Burnett, H. A. Baldis, G. D. Enright, R. Fedosejevs, N. R. Isenor, and I. V. Tomov, *Laser Interaction and Related Plasma Phenomena, Vol. 4A*, edited by H. J. Schwarz and H. Hora (Plenum, New York, 1977), p. 161.
[12] B. L. Henke, J. A. Smith, and D. T. Attwood, Appl. Phys. Lett. **29**, 539 (1976); B. L. Henke, J. A. Smith, and D. T. Attwood, J. Appl. Phys. **48**, 1852 (1977); B. L. Henke and K. Premartne, Jpn. J. Appl. Phys. **17-2**, 477 (1978).
[13] G. L. Stradling, H. Medecki, R. L. Kauffman, D. T. Attwood, and B. L. Henke, Appl. Phys. Lett. **37**, 782 (1980).
[14] P. A. Jaanimagi, N. A. Ebrahim, N. H. Burnett, and C. Joshi, Appl. Phys. Lett. **38**, 734 (1981).
[15] P. A. Jaanimagi and M. C. Richardson, Opt. Commun. **44**, 180 (1983).
[16] H. E. Kulsrud, RCA Rev. **28**, 351 (1967).
[17] B. A. Carre, Comput. J. **4**, 73 (1961).